

## DESIGN CONSIDERATIONS FOR PLANAR INVERTED-F ANTENNA

Hua-Ming Chen<sup>\*</sup>, Hsiu-Hsiung Lin<sup>\*\*</sup>, Ping-Shou Cheng<sup>\*\*</sup> and Yi-Fang Lin<sup>\*</sup>  
<sup>\*</sup>Institute of Photonics and Communications  
 National Kaohsiung University of Applied Sciences, Kaohsiung 807, Taiwan  
 E-mail: hmchen@cc.kuas.edu.tw  
<sup>\*\*</sup>Department of Electronic Engineering  
 National Kaohsiung University of Applied Sciences, Kaohsiung 807, Taiwan

### 1. Introduction

Compact antennas have been the center of interest of much research because of the rapid progress in wireless communications. The low profile, light weight and low fabrication cost make microstrip antenna very attractive for wireless communications. The size of the microstrip antenna, however, may cause inconveniences for wireless applications at the lower microwave frequencies. To reduce the microstrip antenna size, a potential candidate is the planar inverted-F antenna, which is a modified form of the microstrip antenna. The PIFA is a quarter-wavelength shorted patch, which consists of a finite ground plane, a top radiator, a coaxial probe and a shorting mechanism that short the top radiator to the ground plane. There are several shorting mechanism, such as the use of a shorting pin [1-4], a shorting plate [5-8] and a shorting plate together with a shorting pin [9-10].

This paper proposes a planar inverted-F antenna, where an edge of the radiator is terminated with a shorted plate, and fed by a coaxial probe along the centerline of the radiator. This work includes parametric studies of PIFA behavior, involving the shorting plate width, antenna height, input impedance on the radiator and ground plane size. The effects of design parameters of the PIFA on its operational frequency, impedance bandwidth and radiation patterns are presented and discussed.

### 2. Antenna configuration

The configuration of the proposed PIFA is shown in Fig. 1. The rectangular radiating patch made of 0.2 mm copper plate has a dimension of  $L \times W$ ; and is located in the middle of a 0.2 mm thick copper ground plane of dimension  $L_g \times W_g$ . The antenna height  $h$  is filled with an air substrate ( $\epsilon_r = 1.0$ ). The shorting plate consists of a vertical conducting strip with dimension  $W_s \times h$ , and it is used not only to connect between the patch and ground, but also to suppose the whole antenna. The  $50 \Omega$  coaxial probe has a radius with 0.64 mm and is fed in the centerline of the rectangular patch. The distance between the feeding position and the shorting plate is  $d$ . The coaxial feed can excites the PIFA in  $TM_{10}$  mode.

### 3. Experimental results and discussions

Typical proposed antenna were implemented and studied. In the following studies, the size of the radiating patch is selected to be  $L = 30$  mm and  $W = 40$  mm. The ground plane also has the same dimension with  $L_g = 30$  mm and  $W_g = 40$  mm. For a fixed antenna height  $h$  (4 mm), the measured return loss for different shorting plate width is shown in Figure 2 and listed in Table 1 for comparison. It is first found that the width ( $W_s$ ) of the shorting plate is larger than 20 mm and the excited resonant frequency is  $TM_{10}$  mode of the quarter-wave patch (see Fig. 2a). In Fig. 2b, the width ( $W_s$ ) is less than 20 mm, the proposed antenna is excited in half-wave resonance. For the quarter-wave patch, the resonant frequency is increased with increasing the shorting plate width.

Table 1: Performances of the PIFA with various width ( $W_s$ ). Antenna parameters are given in Fig. 2.

Shorting plate width $W_s$ , mm	Feed position $d$ , mm	Resonant frequency $f_c$ , MHz	Bandwidth, %
0	7.5	4610	4.56
5	5.5	4775	4.82
10	7.0	4867	4.01
15	6.5	4905	2.65
20	1.5	1805	2.22
25	3.5	1946	2.26
30	5.5	2106	2.47
35	6.0	2281	3.37
40	5.5	2296	2.48

Figure 3 shows the experimental and simulation results for  $W_s = 20$  mm, 25 mm, 40 mm. The simulation software IE3D was used for optimizing the design parameters. The shift in simulated resonant frequency  $f_c$  is less than 1.5 % in most cases when compared with measurements. By using the simulation software, the excited patch surface current densities are also simulated and analyzed. The simulated current distributions of the two resonant frequencies for  $W_s = 10$  mm and 25 mm are plotted in Figs. 4a and b, respectively. For the case in Fig. 4a, the excited current distribution is very similar to that of the  $TM_{10}$  mode of the half-wave patch, and it is slightly affected by the shorting plate width ( $W_s$ ). As for the case in Fig. 4b, the current distribution of the  $TM_{10}$  mode is strongly perturbed, since the width of the shorting plate is present. Because of the larger shorting plate width, the maximum of the current distribution is close to the shorted edge. The currents find a resonant condition for quarter-wave patch, and the current-line path length decreases with increasing shorting plate width. This is because the resonant frequency increases as the shorting plate width  $W_s$  increases. To design the resonant frequency, simple semi-empirical formulas have been found very useful. An approximate equation is derived by fitting the experimental data (for  $W_s \geq 20$  mm):

$$f_c = \frac{c}{4(L + \Delta L + k_1 \Delta W^2 + k_2 \Delta W)} \quad (1)$$

$$\Delta W = W - W_s, k_1 = 0.0188, k_2 = 0.0767 \quad (2)$$

where  $c$  is the speed of light in free space,  $\Delta L$  is the equivalent over-length for stand rectangular patch [11],  $k_1$ ,  $k_2$  and  $\Delta W$  is a correction factor for the shorting plate effect. The evaluated results of the equation 1 are shown in Fig. 5 for comparison, and the maximum relative difference between resonant frequencies is less than about 0.5%.

The radiation patterns of the proposed antenna in the two principal planes are presented in Fig. 6. It is known that the power is radiated from the shorting plate where the current is concentrated, and the peak power direction is at about  $\theta = -30^\circ$ . In addition, the radiation from the shorting plate leads to a dip in the pattern of  $E_\phi$  (cross polarization) in the x-z plane and  $E_\theta$  (co-polarization) in the y-z plane. Edge diffraction due to a finite ground plane introduces high cross polarization, and the cross polarization is higher than the co-polarization in the y-z plane.

#### 4. Conclusions

A measurements on a finite ground plane mounted PIFA were performed to investigate the effects of the shorting plate width. The results determined by simulations and measurements showed very good agreement. Moreover, a simple and semi-empirical approximate equation has been derived for the accurate design of the resonant frequency of different shorting plate width.

#### 5. References

1. P. Salonen, M. Keskillammi and M. Kivikoski, 'New slot configurations for dual-band planar inverted-F antenna', *Microwave Opt. Technol. Lett.*, vol. 28, no. 5, pp. 293-298,

- 2001.
2. S.H. Yeh, S.T. Fang and K.L. Wong, 'Dual-band shorted patch antenna for dual ISM-band application', *Microwave Opt. Technol. Lett.*, vol. 32, no. 1, pp. 79-80, 2002.
  3. H.T. Chen, K.L. Wong and T.W. Chiou, 'PIFA with a meandered and folded patch for the dual-band mobile phone application', *IEEE Trans. Antennas Propagat.*, vol. 51, no. 9, pp. 2468-2471, 2003
  4. S.H. Yeh, K.L. Wong and T.W. Chiou and S.T. Fang, 'Dual-band planar inverted F antenna for GSM/DCS mobile phones', *IEEE Trans. Antennas Propagat.*, vol. 51, no. 5, pp. 1124-1126, 2003,
  5. M.F. Abedin and M. Ali, 'Modifying the ground plane and its effect on planar inverted-F antennas for mobile phone handsets', *IEEE Antennas and Wireless Propagat. Letters*, vol. 2, pp. 226-229, 2003.
  6. M.C. Huynh and W. Stutzman, 'Ground plane effects on planar inverted-F antenna performance', *IEE Proc.-Microw. Antennas Propagat.*, vol. 150, no. 4, pp. 209-213, 2003.
  7. J.S. Row, 'Experimental studies of the dual-band planar inverted slot antenna with a U-shaped slot', *Microwave Opt. Technol. Lett.*, vol. 37, no. 5, pp. 359-361, 2003.
  8. C.L. Mak, R. Chair, K.F. Lee, K.M. Luk and A.A. Kishk, 'half U-slot patch antenna with shorting wall', *Electron. Lett.*, vol. 39, no. 25, 2003.
  9. H.C. Tung and K.L. Wong, 'A shorted microstrip antenna for 2.4/5.2 GHz dual-band operation', *Microwave Opt. Technol. Lett.*, vol. 30, no. 6, pp. 401-402, 2001.
  - 10 W.C. MOK, R. Chair and K.F. Lee, 'Wideband quarter-wave patch antenna with shorting pin', *IEE Proc.-Microw. Antennas Propagat.*, vol. 150, no. 1, pp. 56-60, 2003,.
  11. R. Garg, P. Bhartia, I. Bahl and A. Ittipiboon, *Microstrip Antenna Design Handbook*, Artech House, Norwood, MA, 2001.

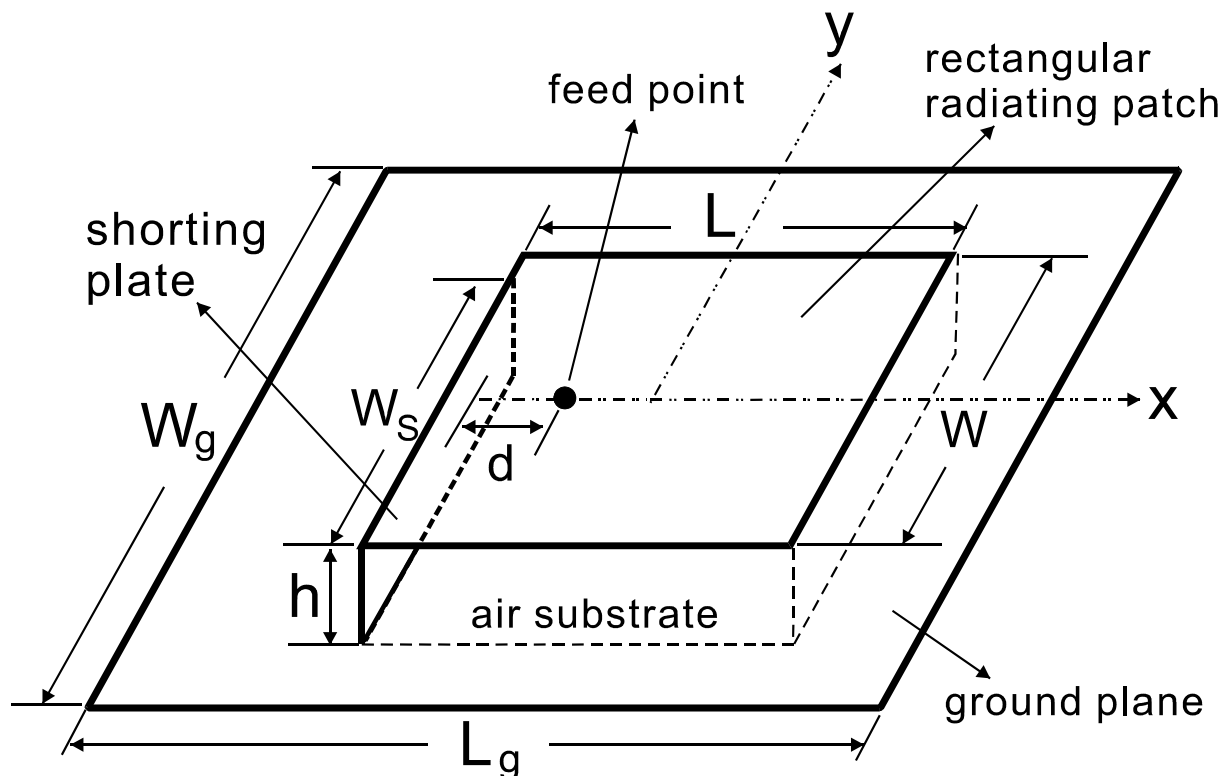


Fig.1 Geometry of a single-feed rectangular microstrip antenna with a shorting plate.

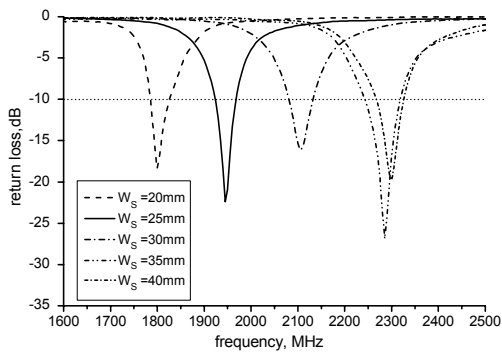


Fig. 2a Measured return loss for the proposed antenna with various shorting plate width ( $W_s$ );  $\epsilon_r = 1.0$ ,  $h = 4.0$  mm,  $L = L_g = 30$  mm,  $W = W_g = 40$  mm.

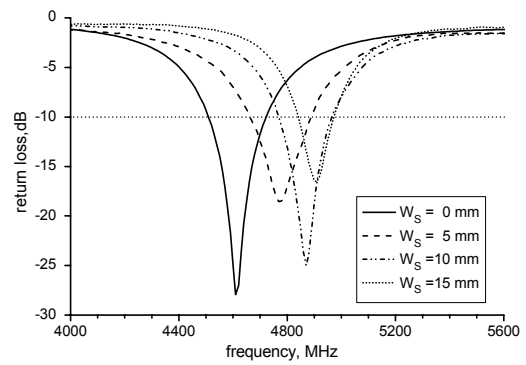


Fig. 2b Measured return loss for the proposed antenna with various shorting plate width ( $W_s$ );  $\epsilon_r = 1.0$ ,  $h = 4.0$  mm,  $L = L_g = 30$  mm,  $W = W_g = 40$  mm.

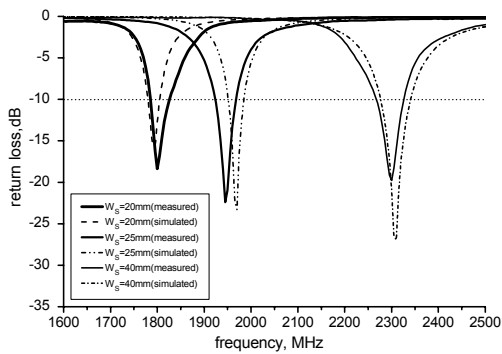


Fig. 3 Measured and simulated return loss for the proposed antenna with various shorting plate width ( $W_s$ ); antenna parameters are given in Fig. 2.

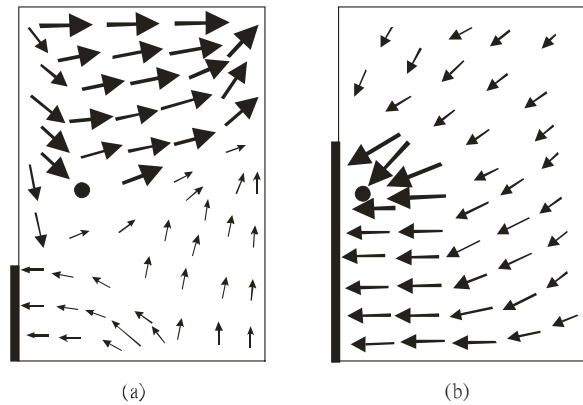


Fig. 4 Simulated current distributions for the proposed design; other antenna parameters are given in Fig. 2. (a)  $W_s = 10$  mm. (b)  $W_s = 25$  mm.

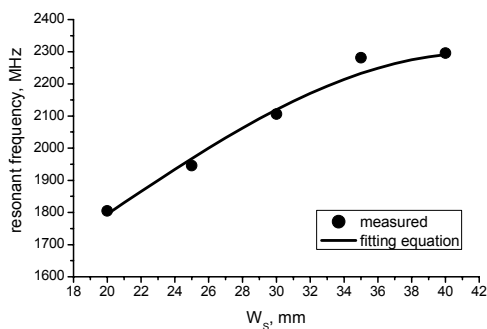


Fig. 5 Comparison of evaluated results of approximate equation and experimental results for various shorting plate width ( $W_s$ ).

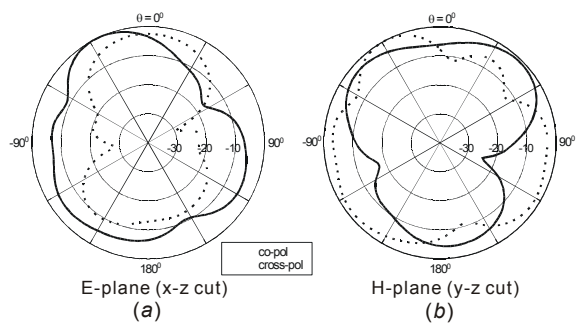


Fig. 6 Measured E-plane (x-z plane) and H-plane (y-z plane) radiation patterns for the proposed design with  $W_s = 25$  mm; antenna parameters are given in Fig. 2.